Coupled sea surface temperature-seawater delta O-18 reconstructions in the Arabian Sea at the millennial scale for the last 35 ka

Coupled sea surface temperature–seawater $\delta^{18}O$ reconstructions in the Arabian Sea at the millennial scale for the last 35 ka

Pallavi Anand,[1,2] Dick Kroon,[3] Arun Deo Singh,[4] Raja S. Ganeshram,[3] Gerald Ganssen,[1] and Henry Elderfield[5]

[1]   Two sediment cores from the western (905; 10.46°9′N, 51.56°4′E, water depth 1586 m) and eastern (SK17; 15°15′N, 72°58′E, water depth 840 m) Arabian Sea were used to study past sea surface temperatures (SST) and seawater $\delta^{18}O$ ($\delta^{18}Ow$) variations for the past 35 ka. We used coupled Mg/Ca-$\delta^{18}O$ calcite variability in two planktonic foraminiferal species: *Globigerinoides ruber*, which thrives throughout the year, and *Globigerina bulloides*, which occurs mainly when surface waters contain high nutrients during upwelling or convective mixing. SSTs in both areas based on Mg/Ca in *G. ruber* were ~3 to 4°C lower during the Last Glacial Maximum (LGM; ~21 ka) than today and the Holocene period. The SST records based on *G. bulloides* also indicate general cooling, down to 18°C in both areas. SSTs in the western Arabian Sea based on *G. bulloides* were always lower than those based on *G. ruber*, indicating the presence of strong seasonal temperature contrast during the Holocene and LGM. We interpret the consistent presence of this seasonal temperature contrast to reflect a combination of seasonal summer upwelling (SW monsoon) and winter convective mixing (NE monsoon) in the western Arabian Sea. In the eastern Arabian Sea, *G. bulloides*-based SSTs were slightly lower (about 1°C) than *G. ruber*-based SSTs during the Holocene, indicating the almost absence of a seasonal temperature gradient, similar to today. However, a large seasonal temperature contrast occurred during the LGM which favors the assumption that strong NE monsoon winds forced winter upwelling or convective mixing offshore Goa. SST and $\delta^{18}Ow$ reconstructions reveal evidence of millennial-scale cycles, particularly in the eastern Arabian Sea. Here, the stadial periods (Northern Hemisphere cold periods such as Younger Dryas and Heinrich events) are marked by increasing SSTs and salty sea surface conditions relative to those during the interstadial periods. Indeed, the $\delta^{18}Ow$ record shows evidence of low-saline surface waters during interstadial periods, indicating increased freshwater runoff from the Western Ghats as a consequence of enhanced SW monsoon intensity.

1.   Introduction

[2]   The monsoon wind system in the Arabian Sea produces distinct seasonal and spatial patterns in surface ocean properties including temperature, circulation, biological productivity and vertical fluxes of biogenic and lithogenic materials. The southwest summer monsoon results from the differential heating and pressure gradients between the tropics and intertropical convergence zone (ITCZ), which lies over central Asia. During this period southwesterly winds drive open ocean upwelling through the Findlater jet and coastal upwelling off Somalia and Oman [*Wyrtki*, 1973; *Clemens et al.*, 1991]. The SW monsoon upwelling in the western Arabian Sea (WAS) brings cold (18−22°C) and nutrient-rich waters from a depth of approximately 200 m to the sea surface [*Peeters et al.*, 2002]. Because of reversal of the wind pattern in winter, the northeast monsoon causes weak and sporadic upwelling along the coasts off India and Pakistan (Eastern Arabian Sea (EAS)). The winter monsoon also causes deep convective mixing across the upper thermocline [*Banse*, 1987], which results in a moderate increase in productivity throughout the basin and decreased sea surface temperature. Thus, the modern sea surface temperature (SST) and salinity (SSS) patterns in the Arabian Sea are seasonal (Figure 1) [*Levitus and Boyer*, 1994]. The upwelling waters in the western sector during summer monsoon are cold and only slightly less saline compared to nonupwelling sea surface conditions during winter. In the eastern sector the presence of low-salinity water due to runoff from summer monsoon prevails during October through March (Figure 1).

[3]   The cold and nutrient-rich surface conditions can be achieved both by upwelling and deep convective mixing during winter cooling as both processes would bring nutrient

---
[1]FALW, Free University, Amsterdam, Netherlands.
[2]Department of Earth Sciences, Open University, Milton Keynes, UK.
[3]School of Geosciences, University of Edinburgh, Edinburgh, UK.
[4]Department of Geology, Banaras Hindu University, Varanasi, India.
[5]Department of Earth Sciences, University of Cambridge, Cambridge, UK.

and cold water from depth to the surface. Upwelling brings subsurface waters to the surface and distributes them laterally [*Blanton*, 1973]. In contrast, convective mixing acts more uniformly across the surface of the basin, bringing waters from below the thermocline and incorporating them locally into the mixed layer [*Labiosa et al.*, 2003]. Both upwelling and winter convection control mixed layer depth and phytoplankton blooms, e.g., in the Gulf of Aqaba [*Labiosa et al.*, 2003].

[4] Numerous studies have shown that the SW monsoon weakened and the NE monsoon intensified during glacial periods [*Prell et al.*, 1980; *Cullen*, 1981; *Duplessy*, 1982; *Fontugne and Duplessy*, 1986; *Sirocko et al.*, 1993; *Sirocko and Ittekkot*, 1992; *Rostek et al.*, 1993, 1997]. Most reconstructions of the Indian monsoon have been based on proxies associated with summer monsoon-induced upwelling in the WAS, e.g., abundance counts and/or isotopic composition in shells of upwelling related planktonic foraminifera [*Prell*, 1984; *Naidu and Malmgren*, 1995; *Anderson et al.*, 2002; *Gupta et al.*, 2003]. Attempts have been made to understand the effect of changing monsoonal strength across the Arabian Sea basin by reconstructing the sea surface temperature, seawater δ^{18}O (δ^{18}Ow) and salinity variations using a combination of alkenone unsaturation ratios and oxygen isotopes in shells of foraminifera [*Rostek et al.*, 1993, 1997; *Reichart et al.*, 2002]. However, the seasonal abundance variations of biogenic producers (proxy carriers) such as planktonic foraminifera and alkenone producing coccoliths may differ and thus the validity of temperature, δ^{18}Ow and salinity reconstructions needs to be confirmed using other approaches.

[5] Recently, a multiproxy approach (Mg/Ca and δ^{18}Ow) on the surface dwelling species *Globigerinoides ruber* (average annual signal) derived temperature and oxygen isotopic compositions of seawater for four time periods (0, 8, 15 and 20 ka) across the Arabian Sea [*Dahl and Oppo*, 2006]. In this study, we have applied the same method, but derived temperature and δ^{18}Ow variations on the basis of two planktonic foraminiferal species *Globigerinoides ruber* and *Globigerina bulloides* from two high-resolution time series: one site in the western sector and one site in the eastern sector of the Arabian Sea for the past 35 ka. By using two species with different ecological behavior we aim to obtain seasonal information on the spatial and temporal variations in seasonal sea surface conditions in the Arabian Sea. Today, *G. bulloides* calcifies primarily during upwelling (high-nutrient conditions), while *G. ruber* thrives all year around (average annual signal of surface conditions). The two core sites were chosen to record the temperature and δ^{18}Ow histories for the past 35 ka in relation to monsoon development. Both sites would have experienced the overall low-latitude, tropical temperature and δ^{18}Ow variations but these signals may have been altered or overprinted by local variations.

2. Core Sites

[6] We studied core 905 from the western Arabian Sea (WAS) off Somalia and core SK17 from the eastern Arabian Sea (EAS) located off Goa. Core 905 is located below the

present-day upwelling cell produced during the SW monsoon. The SW monsoon induces Ekman transport and upwelling of cold and nutrient-rich water offshore Somalia resulting in enhanced biological productivity. Biogenic sedimentation in the WAS is very high approximately 70% of the total annual flux [*Nair et al.*, 1989]. The period of intense upwelling and high productivity is followed by stratified, oligotrophic surface waters of low productivity at the core site 905.

[7] The core site SK17 is situated under the low-salinity plume developed by runoff from the Western Ghats during the summer monsoon [*Sarkar et al.*, 2000]. The area is also under the minor influence of low-salinity water from the eastern Indian Ocean related to summer monsoon runoff into the Bay of Bengal [*Wyrtki*, 1973] which reaches the eastern Arabian Sea in winter (Figure 1) A weak upwelling during the winter season brings slightly cooler and nutrient-rich subsurface water which is marked by increased abundance of *G. bulloides* (~20%) whereas during the summer *G. ruber* (~30%) is the dominant species near the core site [*Zhang*, 1985; *Cullen and Prell*, 1984; *Nair et al.*, 1989].

3. Materials and Methods

[8] Piston core 905 was collected from 10.46°9′N, 51.56°4′E (water depth 1586 m) during the cruise of R/V Tyro on the continental margin off Somalia as part of the Netherlands Indian Ocean Project (NIOP) [*Van Hinte et al.*, 1995]. Gravity core SK17 was raised from the central part of the western continental margin off Goa from 15°15′N, 72°58′E during the ORV Sagar Kanya cruise (Figure 1) at a water depth of 840 m where the present oxygen minimum zone impinges on the continental slope. Core 905 (containing bioturbated homogeneous calcareous ooze) was sampled at 20 cm intervals and core SK17 (composed of intermittently dark colored laminated intervals containing abundant foraminifera and light colored homogeneous layers containing high numbers of pteropod shells [*Singh et al.*, 2006]) was sampled at 4–5 cm intervals for this study. Sediments were disaggregated and washed in ultra-pure water and dried. Foraminiferal samples were sieved and individual specimens of *G. ruber* and *G. bulloides* were handpicked from the size fraction 250–300 μm of core 905 and from the size fraction 250–350 μm of core SK17.

[9] The age models of core 905 and SK17 are based on twelve [*Ivanova*, 2000; *Jung et al.*, 2002] and fourteen AMS ^{14}C dates [*Singh et al.*, 2006], respectively. The details of the age models, calculation of calendar ages (ka), and reservoir effect used are given in the references [*Ivanova*, 2000; *Jung et al.*, 2002; *Singh et al.*, 2006].

3.1. Oxygen Isotope and Mg/Ca Analyses

[10] The foraminiferal samples were gently crushed under glass plates and homogenized for Mg/Ca measurement. Samples for Mg/Ca analyses were chemically cleaned using the method of *Barker et al.* [2003] before analysis by ICP-OES [*de Villiers et al.*, 2002]. Oxygen isotopes of foraminiferal samples were measured on a Finnigan MAT 252 mass spectrometer. At the time of measurement, precision of measured Mg/Ca ratios was <0.02 mmol/mol (1 σ s.d.) for a standard solution of Mg/Ca = 5.13 (mmol/mol) and analytical
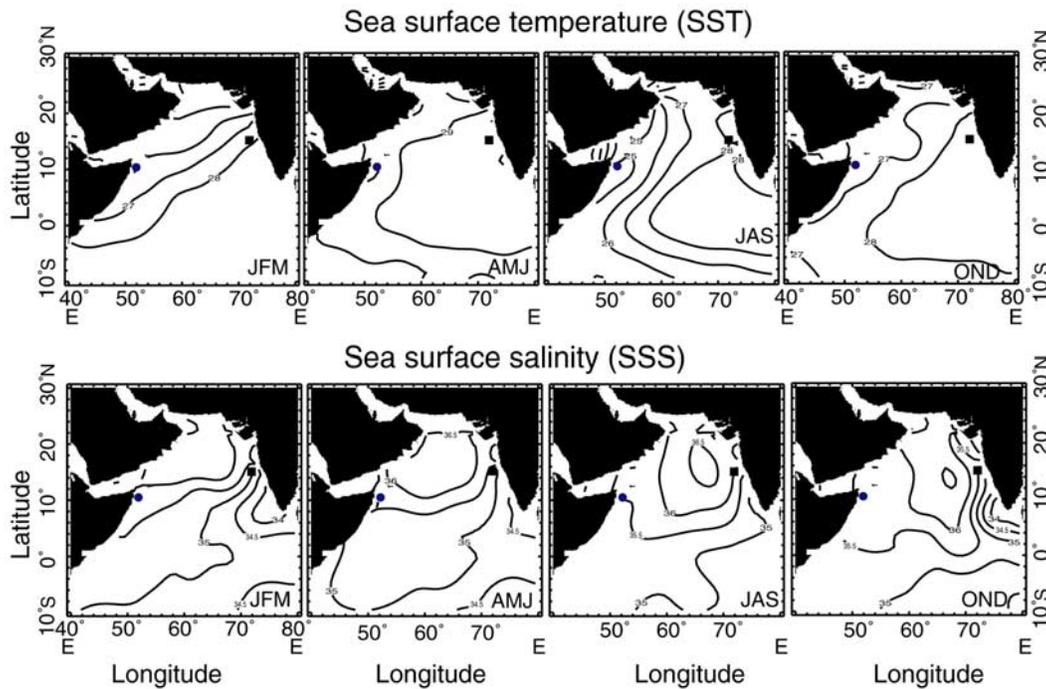
Figure 1. Arabian Sea sea surface temperature (°C) and salinity (practical salinity units (psu)) data for January–February–March (JFM), April–May–June (AMJ), July–August–September (JAS), and October–November–December (OND) are from *Levitus and Boyer* [1994]. The two cores studied are also shown, filled circle (core 905: 10.46°9′N, 51.56°4′E; water depth 1586 m) and filled square (SK17: 15°15′N, 72°58′E; water depth 840 m).

precision for the δ^{18}Oc analyses is better than ±0.06‰. We used *G. ruber* δ^{18}Oc data of core SK17 from *Singh et al.* [2006] and *G. ruber, G. bulloides* δ^{18}Oc data of core 905 from *Ivanova* [2000]. We performed duplicate measurements of δ^{18}Oc of *G. ruber* of core 905 during the Last Glacial Maximum (LGM)-Holocene transition and LGM samples.

3.2. Estimation of Temperature and δ^{18}Ow From Mg/Ca and δ^{18}Oc of Planktonic Foraminifera

[11] Temperature estimates based on Mg/Ca of *G. ruber* and *G. bulloides* were obtained using species-specific equations obtained from Atlantic sediment trap and core top calibrations [*Anand et al.*, 2003; *Elderfield and Ganssen*, 2000] (Figure 3a). The Mg/Ca-temperature equations used in this study are (1) T = (1/0.09)*LN(Mg/Ca/0.449) (see *Anand et al.* [2003] for *G. ruber*) and (2) T = (1/0.102)*LN(Mg/Ca/0.528) (see *Elderfield and Ganssen* [2000] for *G. bulloides*).

[12] We selected these calibration equations because derived temperatures of core tops were close to modern values.

[13] δ^{18}Ow was constructed from δ^{18}Oc using Mg/Ca-temperature as an independent temperature proxy. We applied the following equations to calculate δ^{18}Ow: δ^{18}Ow = 0.27 + δ^{18}Oc + ((T-14.2)/4.81) (see *Peeters* [2000] for *G. bulloides*) and δ^{18}Ow = 0.27 + δ^{18}Oc + ((T-14.9)/4.8)) (see *Bemis et al.* [1998] for *G. ruber*). The derived δ^{18}Ow estimates were corrected for continental ice

volume using *Shackleton*'s [2000] work and presented as δ^{18}OwIce Volume Free (‰) [δ^{18}OwIVF].

4. Results

[14] Oxygen isotope and Mg/Ca records of *G. ruber* and *G. bulloides* from the two cores are shown in Figures 2a, 2b, 2c, and 2d. *G. ruber* δ^{18}Oc ranges from −1.9 to 0.1 ‰ in core 905 and from −2.9 to −0.3 ‰ in core SK17. *G. bulloides* δ^{18}Oc ranges from −1.4 to 0.4 ‰ in core 905 and from −2.7 to −0.1 ‰ in core SK17 (Figures 2a and 2b). Both species show higher Mg/Ca values in core SK17 compared to those in core 905. The *G. ruber* Mg/Ca ranges from 4.6 to 3.3 mmol/mol in core 905 and from 5.6 to 3.4 mmol/mol in core SK17. *G. bulloides* Mg/Ca ranges from 8.2 to 3.3 mmol/mol in core SK17 and from 6.1 to 3.5 mmol/mol in core 905 (Figures 2c and 2d). The glacial-interglacial δ^{18}Oc transition in SK17 is stepwise with a clear reversal around 10–12 ka, while core 905 δ^{18}Oc records show a smooth profile for the same interval. A stepwise transition in core SK17 can also be seen in the Mg/Ca (mmol/mol) profile, although it is out of phase with the δ^{18}Oc transition. For instance, the main step in Mg/Ca (midpoint) occurred at 17 ka, while in δ^{18}Oc it occurred at 14 ka.

[15] The Holocene Mg/Ca-sea surface temperature (SST) records from the EAS and WAS show that (Figures 3a and 3b) (1) average Holocene SSTs (*G. ruber*) were warmer in
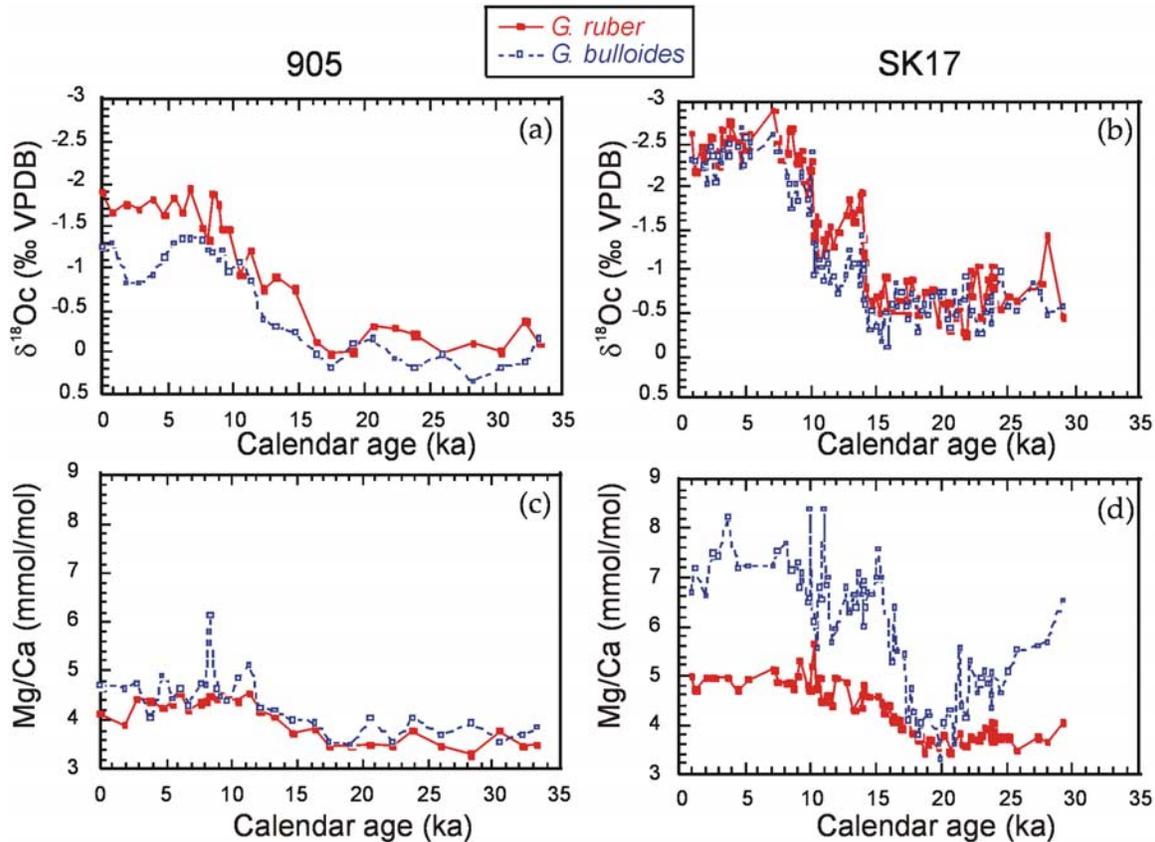
Figure 2. Results of (a, b) δ^{18}Oc (‰) and (c, d) Mg/Ca (mmol/mol) of *G. ruber* (Figures 2a and 2c) and *G. bulloides* (Figures 2b and 2d) from core 905 and SK17 for the past 35 ka.

the EAS compared to WAS, (2) *G. bulloides* calcified in cooler waters in the WAS compared to EAS, and (3) The seasonal SST contrast was much stronger in the WAS compared to EAS (difference in the SSTs of *G. ruber* and *G. bulloides*).

[16] The results of Mg/Ca sea surface temperature records of glacial to Holocene timescales for the EAS and WAS show that (Figures 3a and 3b) (1) the *G. ruber* (average annual SST of ∼23°C) and *G. bulloides* (upwelling SST of ∼18°C) Mg/Ca SSTs are about the same at both sites during the LGM, (2) the average annual SST difference between LGM and Holocene was ∼3°C and ∼4°C on the basis of *G. ruber* Mg/Ca SST estimates in the WAS and EAS, respectively, (3) *G. bulloides* temperature records off Somalia suggest 3°C cooling during the LGM, and (4) *G. bulloides* Mg/Ca SST records of the EAS show cooling of ∼4°C–5°C during the LGM compared to the Holocene.

[17] The SSTs based on both species show a tendency to increase during the stadial periods (Northern Hemisphere cold periods), particularly during the time of Heinrich event 1 (Figures 3a and 3b). The δ^{18}OwIVF reconstructions based on both species show evidence of millennial-scale variability in the EAS (Figures 3c and 3d). Such evidence is not clear in the core 905 δ^{18}OwIVF records, perhaps because of the low sample resolution of 1 ka per sample (Figures 3c and 3d). The δ^{18}OwIVF records in the EAS reveal evidence

of salty water conditions during stadial periods (Northern Hemisphere cold periods compared to the less salty conditions during interstadial periods (Northern Hemisphere warm periods)), similar to those of the Holocene (Figure 3d).

5. Discussion

5.1. Temperature Records

5.1.1. Holocene

[18] The average Holocene annual SSTs based on *G. ruber* shells were slightly colder at the location of core 905 (WAS) compared to core SK17 (EAS). This can be explained by the influence of strong seasonal upwelling in the WAS during summer and more or less stratification of surface waters in the EAS. The seasonal cooling, controlled by upwelling, [*Wyrtki*, 1973] only partially influenced Holocene *G. ruber* temperature values because it calcifies in both monsoonal seasons in the WAS [*Peeters et al.*, 2002]. However, the *G. bulloides*-based SSTs are much colder than the *G. ruber* SSTs supporting the interpretation that *G. bulloides* calcifies mainly in upwelled waters during the SW summer monsoon off Somalia [*Peeters et al.*, 2002].

[19] The *G. bulloides* SSTs are about 1°C lower than the *G. ruber*-based SSTs in core SK17 (EAS) during the Holocene. This can be best explained by a minor SST
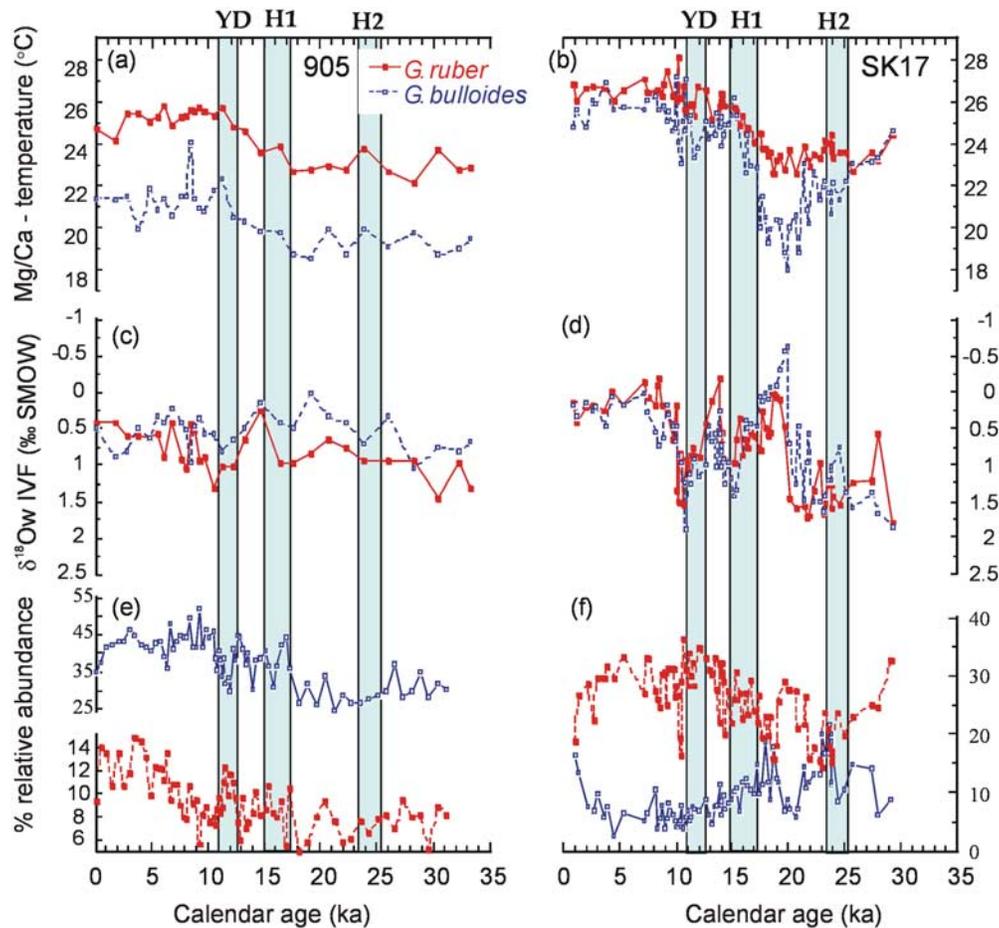
Figure 3. (a, b) Mg/Ca-temperature (°C), (c, d) seawater δ^{18}O (‰ standard mean ocean water) corrected for global ice volume (Ice Volume Free = δ^{18}OwIVF) [*Shackleton*, 2000], and (e, f) percent relative abundance records of *G. ruber* (red) (Figures 3a, 3c, and 3e) and *G. bulloides* (blue) (Figures 3b, 3d, and 3f) from core 905 and SK17 for the past 35 ka. The δ^{18}O of seawater is calculated using Mg/Ca-temperature and δ^{18}O of foraminiferal calcite and corrected for global ice volume using *Shackleton*'s [2000] curve. The shaded bars on SK17 and 905 plots show timing and duration of Younger Dryas (YD), Heinrich 1 (H1), and Heinrich 2 (H2) events in the North Atlantic [*Bard and Kromer*, 1995].

seasonal contrast in this area during this period, similar to today [*Cullen and Prell*, 1984; *Zhang*, 1985]. Minor upwelling during the summer or winter seasons or convective mixing caused a small fall in sea surface temperatures and moderate increase of nutrients for *G.bulloides* to thrive on.

5.1.2. Glacial-Early Holocene

[20] The reconstructed SSTs based on *G. bulloides* (~18°C) and *G. ruber* (~23°C) at the two sites are similar during the Last Glacial Maximum (LGM; ~21 Ka) (Figures 3a and 3b). The *G. ruber* average annual temperatures were ~3 to 4°C lower during the LGM than today and the Holocene period. The extent of cooling during the LGM observed in this study is much greater than observed on the basis of the foraminiferal transfer function (1°C) [*CLIMAP Project Members*, 1981] or other studies [*Cayre and Bard*, 1999; *Naidu and Malmgren*, 2005]. However, a 3°C–4°C LGM SST cooling is in agreement with results from studies based on alkenones [*Rostek et al.*, 1993, 1997; *Emeis et al.*,

1995; *Bard et al.*, 1996; *Reichart et al.*, 2002; *Higginson et al.*, 2004] and Tex$_{86}$ [*Huguet et al.*, 2006]. The LGM Mg/Ca-SST estimates of *G. ruber* (~23°C) derived from this study are similar to the Mg/Ca SSTs (at 20 ka) as reported by *Dahl and Oppo* [2006] and *Saher et al.* [2007] in nearby cores.

[21] The SST records of the two species show a large difference in temperature in the WAS and the EAS during the LGM, suggesting a large seasonal contrast in both areas (Figures 3a and 3b). The relatively cold temperatures of *G. bulloides* suggest that seasonal upwelling and/or deep convective mixing, both processes bringing up nutrients, may have occurred. However, the timing and intensity of the upwelling and/or deep convective mixing during the seasons and associated monsoon winds may have been different in both areas.

[22] In the WAS the seasonal temperature contrast may be explained by continued summer upwelling (SW monsoon),

similar to today, and/or may have been caused by deep convective mixing during winter. Planktonic foraminiferal abundances suggest that relatively less vigorous summer upwelling occurred during the LGM than during the Holocene and today [*Prell et al.*, 1980; *Anderson and Prell*, 1993; *Jung et al.*, 2002] (Figure 3a). However, the *G. bulloides* temperature record does not show the expected relative warming (reduced SST seasonal contrast) with respect to the *G. ruber* SSTs, and thus reduced upwelling cannot entirely explain the observed SST patterns (Figure 3a). The winter NE monsoon winds probably also played a role in maintaining the cold *G. bulloides*-based SSTs through deep convection in addition to the summer upwelling. Previous studies showed that the NE monsoon winds intensified during the LGM [*Fontugne and Duplessy*, 1986; *Rostek et al.*, 1993, 1997] and these winds may have stirred the upper ocean in the entire Arabian Sea basin including the core 905 location.

[23] The large seasonal temperature contrast as found in the Mg/Ca records in SK17 from the eastern Arabian Sea suggests that the strong NE monsoon winds may have caused intense upwelling and/or deep convective mixing offshore Goa. Today and in the Holocene there is weak upwelling in this area during winter [*Zhang*, 1985]. Intense upwelling and/or deep convective mixing turned on during the LGM and may well have lowered the sea surface temperatures during winter. This is consistent with high *G. bulloides* abundances in core SK17 and other upwelling species *Globigerinita glutinata* and *Neogloboquadrina dutertrei*, reflecting elevated nutrient levels [*Singh et al.*, 2006; *Conan and Brummer*, 2000; A. D. Singh, unpublished data, 2008].

5.1.3. Millennial Scale

[24] The SST estimates of *G. ruber* and *G. bulloides* in the EAS and to a lesser extent in the WAS, show warming during the stadial periods (Heinrich event 1 (H1) and Younger Dryas (YD)) (Figure 3b). Similar features were also observed by *Saher et al.* [2007] in nearby core 929 in the WAS. Thus the warming observed during H1 and YD is of regional extent and may have a tropical origin [*Saher et al.*, 2007]. Alternatively, NE monsoon-induced winter deep convective mixing and/or upwelling were reduced across the Arabian Sea. A reduced nutrient content of surface waters is also evident in the foraminiferal abundance records: *G. bulloides* numbers fell and relative *G. ruber* abundance increased (Figure 3f).

5.2. Seawater δ^{18}O Records

[25] Changes in foraminiferal δ^{18}Oc are controlled mainly by global variations of δ^{18}Ow because of the growth of continental ice sheets at the glacial-interglacial timescale and, additionally by local sea surface temperature and evaporation-precipitation (E-P) changes. Sea surface salinity and δ^{18}Ow are directly linked to the local E-P balance, and in general a good linear correlation can be found between these parameters for most of the global ocean [*Craig and Gordon*, 1965] (data are available at http://data.giss.nasa.gov/o18data).

[26] Reconstructions of δ^{18}OwIVF (after ice volume correction) from the two sites show large fluctuations in δ^{18}OwIVF in the eastern sector (SK17) compared to the western sector (905) of the Arabian Sea (Figures 3c and 3d). At the site of core 905, we observe small or no changes in δ^{18}OwIVF. The eastern Arabian Sea δ^{18}OwIVF records of both species reveal three episodes characterized by high δ^{18}OwIVF values centered at 23 ka, 16 ka and 11 ka (Figure 3d). These heavy δ^{18}OwIVF signals are observed during periods when North Atlantic surface waters experienced strong cooling (e.g., the H2, H1 and YD events) (Figure 3d) [*Ruddiman and McIntyre*, 1981, *Bard et al.*, 1987; *Karpuz and Jansen*, 1992]. *Anderson and Thunell* [1993] suggested that δ^{18}Oc transient events in the tropics were related to changes in the δ^{18}OwIVF and not to the cooling of sea surface temperature. This was also supported by work of *Bard et al.* [1996] showing that cooling was minimal during δ^{18}O transient events in the Indian Ocean. Our results support this interpretation that when the North Atlantic was cold, SST changes in the tropics were minimal or even marked by warming as observed in the Arabian Sea (Figure 3b [see also *Saher et al.*, 2007], in the WAS) and thus the δ^{18}OwIVF changes have a different origin.

[27] Given the location of this site we suggest that the δ^{18}OwIVF changes in the eastern Arabian Sea are related to monsoon intensity changes. The SW monsoon brings rainfall to the Western Ghats. It is well known that reduced productivity occurred in the western and northern Arabian Sea when the North Atlantic sea surface waters were cool at the millennial scale and thus the SW monsoon was reduced during stadial periods [e.g., *Altabet et al.*, 1995; *Schulz et al.*, 1998, *Ivanochko et al.*, 2005]. Thus the Western Ghats must have received less rainfall and hence surface waters in the EAS received reduced runoff off Goa (core SK17). This has led to increased δ^{18}OwIVF values as evidenced in the SK17 record during the equivalent periods of YD, H1 and H2. Thus, the SW monsoon intensity responded strongly to the temperature history in the North Atlantic highlighting the teleconnections between the two areas.

[28] The lightest δ^{18}OwIVF signal occurred around 19–20 ka (LGM) which is more prominent in the *G. bulloides* than in the *G. ruber* record (Figure 3d). The *G. ruber* δ^{18}OwIVF value during the LGM is very similar to the present-day value but the *G. bulloides* δ^{18}OwIVF is ∼0.5‰ lighter (Figure 3d). The lightest δ^{18}OwIVF event is also accompanied by the coldest temperature during the LGM in *G. bulloides* (Figures 3b and 3d). The present-day δ^{18}Ow values at the core site are influenced by runoff from the Western Ghats during the SW monsoon [*Sarkar et al.*, 2000]. During the LGM the SW monsoon was weakened and thus decreased precipitation leading to reduced runoff from Western Ghats. Therefore, we turn to the other possibility that the cold and light δ^{18}Ow conditions during the LGM were caused by enhanced winter NE monsoon. These winds induced mixing (upwelling + convective mixing) of possible southern source water present at intermediate depths (∼200 m or deeper) in the EAS. The enhanced NE monsoon in winter during the LGM could have resulted into the advection of deep, cold and low-salinity water in the EAS. This scenario can very well be interpreted from the observations recorded in the EAS during the LGM: (1) the increased seasonality from the temperature records of two planktonic

species (Figure 3b), (2) cold (temperature record, Figure 3b) and fresher (δ^{18}OwIVF record, Figure 3d) conditions from *G. bulloides*, (3) a small dip in the abundance of *G. bulloides* together with increased abundance of other marginal upwelling species, e.g., *G. glutinata* [*Singh et al.*, 2006], and (4) peak in abundance of *N. dutertrei* (a cool subsurface dweller planktonic species) (A. D. Singh, unpublished data, 2008). During the LGM the overall water column salinity gradient was weak in the Arabian Sea as there was no high-salinity water outflow from Red Sea and Persian Gulf [*Rohling and Zachariasse*, 1996; *Sirocko*, 2003], which were possibly replaced by northward movement of southern source waters at the intermediate level. The strong wind speed during LGM would have allowed stronger wind induced mixing than present-day [*Nair et al.*, 1989]. Therefore the combined effect of the absence of saline outflow and seasonal upwelling due to intensified NE monsoon related advection of subsurface water are the key factors for the light δ^{18}OwIVF and cold temperature observed in the EAS.

6. Conclusions

[29] The temperature reconstructions using Mg/Ca of foraminifera, *G. ruber* and *G. bulloides* in cores from the EAS and WAS show (1) an average annual temperature (based on *G. ruber*) difference of 3°C–4°C between the LGM and the Holocene in both areas; (2) in the EAS increased seasonal contrast in temperature occurred during the LGM (∼4°C) compared to the Holocene and today (∼1°C), suggesting that upwelling and/or deep convective mixing lowered SSTs during the NE monsoon; (3) in the WAS a large seasonal temperature contrast was maintained during the LGM similar to the Holocene and today, caused by summer upwelling and most likely winter mixing; and (4) Warming occurred during the stadial periods (Northern Hemisphere cold events, e.g., Younger Dryas and Heinrich events).

[30] In the EAS the coupled δ^{18}Oc-temperature reconstructions show heavy δ^{18}OwIVF values during the Younger Dryas and Heinrich events caused by reduced SW monsoon rainfall and runoff from the Western Ghats.

References

Altabet, M. A., D. Francois, W. Murray, and W. L. Prell (1995), Climate-related variations in denitrification in the Arabian Sea from ¹⁵N/¹⁴N ratios, *Nature*, *373*, 506–509, doi:10.1038/373506a0.

Anand, P., H. Elderfield, and M. H. Conte (2003), Calibration of Mg/Ca thermometry in planktonic foraminifera from a sediment trap time series, *Paleoceanography*, *18*(2), 1050, doi:10.1029/2002PA000846.

Anderson, D. M., and W. L. Prell (1993), A 300 kyr record of upwelling off Oman during the late Quaternary: Evidence of the Asian southwest monsoon, *Paleoceanography*, *8*, 193–208, doi:10.1029/93PA00256.

Anderson, D. M., and R. C. Thunell (1993), The oxygen-isotopic composition of tropical ocean surface water during the last deglaciation, *Quat. Sci. Rev.*, *12*, 465–473, doi:10.1016/S0277-3791(05)80010-1.

Anderson, D. M., J. T. Overpeck, and A. K. Gupta (2002), Increase in the Asian southwest monsoon during the past four centuries, *Science*, *297*, 596–599, doi:10.1126/science.1072881.

Banse, K. (1987), Seasonality of phytoplankton cholorophyll in the central and northern Arabian Sea, *Deep Sea Res., Part A*, *34*, 713–723, doi:10.1016/0198-0149(87)90032-X.

Bard, E., and B. Kromer (1995), The Younger Dryas: Absolute and radiocarbon chronology, in *The Younger Dryas*, edited by S. R. Troelstra, J. E. van Hinte, and G. M. Ganssen, *Proc. R. Dutch Acad. Sci.*, *44*, 161–166.

Bard, E., M. Arnold, P. Maurice, J. Duprat, J. Moyes, and J. C. Duplessy (1987), Retreat velocity of the North-Atlantic polar front during the last deglaciation determined by ¹⁴C accelerator mass spectrometry, *Nature*, *328*, 791–794.

Bard, E., F. Rostek, and C. Sonzogni (1996), Interhemispheric synchrony of the last deglaciation inferred from alkenone palaeothermometry, *Nature*, *382*, 241–244, doi:10.1038/382241a0.

Barker, S., M. Greaves, and H. Elderfield (2003), A study of cleaning procedures used for foraminiferal Mg/Ca paleothermometry, *Geochem. Geophys. Geosyst.*, *4*(9), 8407, doi:10.1029/2003GC000559.

Bemis, B., H. Spero, J. Bijma, and D. W. Lea (1998), Reevaluation of the oxygen isotopic composition of planktonic foraminifera: Experimental results and revised paleotemperature equations, *Paleoceanography*, *13*, 150–160, doi:10.1029/98PA00070.

Blanton, J. G. (1973), Vertical entrainment into the epilimnion of stratified lakes, *Limnol. Oceanogr.*, *18*, 697–701.

Cayre, O., and E. Bard (1999), Planktonic foraminiferal and alkenone records of the last deglaciation from the eastern Arabian Sea, *Quat. Res.*, *52*, 337–342, doi:10.1006/qres.1999.2083.

Clemens, S., W. L. Prell, D. Murray, G. B. Shimmield, and G. Weedon (1991), Forcing mechanisms of the Indian Ocean monsoon, *Nature*, *353*, 720–725, doi:10.1038/353720a0.

CLIMAP Project Members (1981), Seasonal reconstruction of the Earth's surface at the Last Glacial Maximum, *Map Chart Ser. MC-36*, Geol. Soc. of Am., Boulder, Colo.

Conan, S. M. H., and G.-J. A. Brummer (2000), Fluxes of planktic foraminifera in response to monsoonal upwelling on the Somalia Basin margin, *Deep Sea Res., Part II*, *47*, 2207–2227.

Craig, H., and L. I. Gordon (1965), Deuterium and oxygen-18 variations in the ocean and atmosphere, in *Stable Isotopes in Oceanographic Studies and Palaeo- Temperatures*, edited by E. Tongiorgi, pp. 9–130, Lab. Geol. Nucl., Pisa, Italy.

Cullen, J. L. (1981), Microfossil evidence for changing salinity patterns in the Bay of Bengal over the last 20,000 years, *Palaeogeogr. Palaeoclimatol. Palaeoecol.*, *35*, 315–356, doi:10.1016/0031-0182(81)90101-2.

Cullen, J. L., and W. L. Prell (1984), Planktonic foraminifera of the northern Indian Ocean: Distribution and preservation in surface sediments, *Mar. Micropaleontol.*, *9*, 1–52, doi:10.1016/0377-8398(84)90022-7.

Dahl, K. A., and D. W. Oppo (2006), Sea surface temperature pattern reconstructions in the Arabian Sea, *Paleoceanography*, *21*, PA1014, doi:10.1029/2005PA001162.

de Villiers, S., M. J. Greaves, and H. Elderfield (2002), An intensity ratio calibration method for the accurate determination of Mg/Ca and Sr/Ca of marine carbonates by ICP-AES, *Geochem. Geophys. Geosyst.*, *3*(1), 1001, doi:10.1029/2001GC000169.

Duplessy, J. C. (1982), Glacial to interglacial contrasts in the northern Indian Ocean, *Nature*, *295*, 494–498, doi:10.1038/295494a0.

Elderfield, H., and G. M. Ganssen (2000), Past temperature and δ^{18}O of surface water inferred from foraminiferal Mg/Ca ratios, *Nature*, *405*, 442–445, doi:10.1038/35013033.

Emeis, K.-C., D. M. Anderson, H. Doose, D. Kroon, and D. Schulz-Bull (1995), Sea-surface temperatures and the history of monsoon upwelling in the northwest Arabian during the last 500,000 years, *Quat. Res.*, *43*, 355–361, doi:10.1006/qres.1995.1041.

Fontugne, M. R., and J. C. Duplessy (1986), Variations of the monsoon regime during the upper Quaternary: Evidence from the carbon isotopic record of organic matter in north Indian Ocean sediments, *Palaeogeogr. Palaeo-*

climatol. Palaeoecol., *56*, 69–88, doi:10.1016/0031-0182(86)90108-2.

Gupta, A. K., D. M. Anderson, and J. T. Overpeck (2003), Abrupt changes in the Asian southwest monsoon during the Holocene and their links to the North Atlantic Ocean, *Nature*, *421*, 354–357, doi:10.1038/nature01340.

Higginson, M. J., M. A. Altabet, L. Wincze, T. D. Herbert, and D. W. Murray (2004), A solar (irradiance) trigger for millennial-scale abrupt changes in the southwest monsoon?, *Paleoceanography*, *19*, PA3015, doi:10.1029/2004PA001031.

Huguet, C., J. -H. Kim, J. S. S. Damste, and S. Schouten (2006), Reconstruction of sea surface temperature variations in the Arabian Sea over the last 23 kyr using organic proxies (TEX86) and UK'37), *Paleoceanography*, *21*, PA3003, doi:10.1029/2005PA001215.

Ivanochko, T. S., R. S. Ganeshram, G.-J. A. Brumer, G. Ganssen, S. J. A. Jung, S. G. Moreton, and D. Kroon (2005), Variations in tropical convection as an amplifier of global climate change at the millennial scale, *Earth Planet. Sci. Lett.*, *235*, 302–314, doi:10.1016/j.epsl.2005.04.002.

Ivanova, E. M. (2000), Late Quaternary monsoon history and paleoproductivity of the western Arabian Sea, Ph.D. thesis, Free Univ., Amsterdam.

Jung, S. J. A., G. R. Davies, G. M. Ganssen, and D. Kroon (2002), Centennial-millennial scale monsoon variations off Somalia over the last 35 kyr, in *Tectonic and Climatic Evolution of the Arabian Sea Region*, edited by P. Clift and D. Kroon, *Spec. Publ. Geol. Soc. London*, *195*, 341–352.

Karpuz, N. K., and E. Jansen (1992), A high-resolution diatom record of the last deglaciation from the SE Norwegian Sea: Documentation of rapid climate changes, *Paleoceanography*, *7*, 499–520, doi:10.1029/92PA01651.

Labiosa, R. G., K. R. Arrigo, A. Genin, S. G. Monismith, and G. van Dijken (2003), The interplay between upwelling and deep convective mixing in determining the seasonal phytoplankton dynamics in the Gulf of Aqaba: Evidence from SeaWiFS and MODIS, *Limnol. Oceanogr.*, *48*, 2355–2368.

Levitus, S., and T. P. Boyer, (1994), *World Ocean Atlas 1994*, vol. 4, *Temperature, NOAA Atlas NESDIS*, vol. 4, 129 pp., NOAA, Silver Spring, Md.

Naidu, P. D., and B. A. Malmgren (1995), Monsoon upwelling effects on test size of some planktonic foraminiferal species from the Oman Margin, Arabian Sea, *Paleoceanography*, *10*, 117–122.

Naidu, P. D., and B. A. Malmgren (2005), Seasonal sea surface temperature contrast between the Holocene and last glacial period in the western Arabian Sea (Ocean Drilling Project Site 723A): Modulated by monsoon upwelling, *Paleoceanography*, *20*, PA1004, doi:10.1029/2004PA001078.

Nair, R. R., V. Ittekkot, S. J. Manganini, V. Ramaswamy, B. Haake, E. T. Degens, B. N. Desai, and S. Honjo (1989), Increased particle flux to the deep ocean related to monsoons, *Nature*, *338*, 749–751, doi:10.1038/338749a0.

Peeters, F. J. C. (2000), The distribution and stable isotope composition of living planktic foraminifera in relation to seasonal changes in the Arabian Sea, Ph.D. thesis, Free Univ., Amsterdam.

Peeters, F. J. C., G. A. Brummer, and G. Ganssen (2002), The effect of upwelling on the distribution and stable isotope composition of *Globigerinoides bulloides* and *Globigerinoides ruber* (planktic foraminifera) in modern surface waters of the NW Arabian sea, *Global Planet. Change*, *34*, 269–291, doi:10.1016/S0921-8181(02)00120-0.

Prell, W. L. (1984), Variation of monsoonal upwelling: A response to changing solar radiation, in *Climate Processes and Climate Sensitivity, Geophys. Monogr. Ser.*, *29*, edited by J. Hansen and T. Takahashi, pp. 48–57, AGU, Washington, D. C.

Prell, W. L., W. H. Hutson, D. F. Williams, A. W. H. Be, K. Geitzenauer, and B. Molfino (1980), Surface circulation of the Indian Ocean during the last glacial maximum: Approximately 18,000 ye BP, *Quat. Res.*, *14*, 309–336, doi:10.1016/0033-5894(80)90014-9.

Reichart, G. J., S. J. Schenau, G. J. De Lange, and W. J. Zachariasse (2002), Synchroneity of oxygen minimum zone intensity on the Oman and Pakistan margins at sub-Milankovitch timescales, *Mar. Geol.*, *185*, 403–415, doi:10.1016/S0025-3227(02)00184-6.

Rohling, E. J., and W. J. Zachariasse (1996), Red Sea outflow during the last glacial maximum, *Quat. Int.*, *31*, 77–83.

Rostek, F., G. Ruhland, F. C. Bassinot, P. J. Muller, L. D. Labeyrie, Y. Lancelot, and E. Bard (1993), Reconstructing sea surface temperature and salinity using δ^{18}O and alkenone records, *Nature*, *364*, 319–321, doi:10.1038/364319a0.

Rostek, F., E. Bard, L. Beaufort, C. Sonzogni, and G. Ganssen (1997), Sea surface temperature and productivity records for the past 240 kyr in the Arabian Sea, *Deep Sea Res., Part II*, *44*, 1461–1480, doi:10.1016/S0967-0645(97)00008-8.

Ruddiman, W. F., and A. McIntyre (1981), The North Atlantic Ocean during the last deglaciation, *Palaeogeogr. Palaeoclimatol. Palaeoecol.*, *35*, 145–214, doi:10.1016/0031-0182(81)90097-3.

Saher, M. H., S. J. A. Jung, H. Elderfield, M. J. Greaves, and D. Kroon (2007), Sea surface temperatures of the western Arabian Sea during the last deglaciation, *Paleoceanography*, *22*, PA2208, doi:10.1029/2006PA001292.

Sarkar, A., R. Ramesh, B. L. K. Somayajulu, R. Agnihotri, A. J. T. Jull, and G. S. Burr (2000), High resolution Holocene monsoon record from the eastern Arabian Sea, *Earth Planet. Sci. Lett.*, *177*, 209–218, doi:10.1016/S0012-821X(00)00053-4.

Schulz, H., U. von Rad, and H. Erlenkeuser (1998), Correlation between Arabian Sea and Greenland climate oscillations of the past 110,000 years, *Nature*, *393*, 54–57.

Shackleton, N. J. (2000), The 100,000-year ice-age cycle identified and found to lag temperature, carbon dioxide, and orbital eccentricity, *Science*, *289*, 1897–1902, doi:10.1126/science.289.5486.1897.

Singh, A. D., D. Kroon, and R. S. Ganeshram (2006), Millennial scale variations in productivity and OMZ intensity in the Eastern Arabian Sea, *J. Geol. Soc. India*, *68*, 369–378.

Sirocko, F. (2003), Ups and downs in the Red Sea, *Nature*, *423*, 813–814, doi:10.1038/423813a.

Sirocko, F., and V. Ittekkot (1992), Organic carbon accumulation rates in the Holocene and glacial Arabian Sea: Implications for O$_2$ consumption in the deep sea and atmospheric CO$_2$ variations, *Clim. Dyn.*, *7*, 162–172, doi:10.1007/BF00206858.

Sirocko, F., M. Sarnthein, H. Erlenkeuser, H. Lange, M. Arnold, and J. C. Duplessy (1993), Century-scale events in monsoonal climate over the past 24,000 years, *Nature*, *364*, 322–324, doi:10.1038/364322a0.

Van Hinte, J. E., T. C. E. van Weering, and S. R. Troelstra (1995), Tracing a seasonal upwelling, report, 146 pp., Natl. Mus. of Nat. Hist., Leiden, Netherlands.

Wyrtki, K. (1973), Physical oceanography of the Indian Ocean, in *The Biology of the Indian Ocean*, edited by B. Zeitzschel and S. A. Gerlach, pp. 18–36, Springer, New York.

Zhang, J. (1985), Living planktonic foraminifera from the eastern Arabian Sea, *Deep Sea Res., Part A*, *32*, 789–798, doi:10.1016/0198-0149(85)90115-3.

————————————

P. Anand and G. Ganssen, FALW, Free University, Amsterdam NL-1081 HV, Netherlands. (pallavi.anand@open.ac.uk)

H. Elderfield, Department of Earth Sciences, University of Cambridge, Cambridge CB2 1TN, UK.

R. S. Ganeshram and D. Kroon, School of Geosciences, University of Edinburgh, Edinburgh EH8 9YL, UK.

A. D. Singh, Department of Geology, Banaras Hindu University, Varanasi 221005, India.